

Full Length Research Paper

Lateral torsional buckling of rectangular beams using variational iteration method

Seval Pinarbasi

Department of Civil Engineering, Kocaeli University, Umuttepe Campus, 41380, Kocaeli, Turkey.
E-mail: sevalp@gmail.com. Tel: +90 262 303 3274.

Accepted 15 March, 2011

Lateral torsional buckling is the main failure mode that controls the design of “slender” beams; that is, the beams which have greater major axis bending stiffness than minor axis bending stiffness or the beams which have considerably large laterally unsupported lengths. Since the buckling equations for beams are usually much more complex than those for columns, most of the analytical studies in literature on beam buckling are concentrated on simple cases. This paper shows that complex beam buckling problems, such as lateral torsional buckling of narrow rectangular cantilever beams whose minor axis flexural and torsional rigidities vary exponentially along their lengths, can successfully be solved using variational iteration method (VIM). The paper also investigates the effectiveness of three VIM algorithms, two of which have been proposed very recently in solving lateral torsional buckling equations. Analysis results show that all iteration algorithms yield exactly the same results in all studied problems. As far as the computation times and spaces are concerned, however, one of these algorithms, called variational iteration algorithm II, is found to be superior than the others especially in lateral torsional buckling problems where the beam rigidities vary along the beam length.

Key words: Lateral torsional buckling, narrow rectangular beam, tapered beam, variable rigidity, variational iteration algorithms, variational iteration method.

INTRODUCTION

Beams are main structural elements which primarily support transverse loads, that is, loads perpendicular to their axes. They are also called flexural members since they are typically designed to carry flexural loads, that is, transverse shear forces and bending moments. As the normal force in a beam is generally negligibly small, the design of a “laterally-braced” beam is usually straightforward: select the most economical “compact” cross section which has adequate major axis section modulus to safely carry maximum bending moment in the beam with adequate web area to carry maximum shear force. However, similar to a slender column which buckles under compressive loads, a “laterally-unbraced” slender beam can also buckle under flexural loads. This occurs due to the fact that when subjected to bending moments, compressive stresses develop at one part of the beam

cross section which tends to buckle in lateral (out-of plane) direction. In such a buckling mode, the beam not only displaces laterally but also twists due to the fact that the remaining part of the beam cross section, which is subjected to tensile stresses, resists against buckling. For this reason, this buckling mode is commonly called “lateral torsional buckling”. Lateral torsional buckling, or simply lateral buckling, is the main limit state that has to be considered in the design of “slender” beams, that is, the beams which have greater stiffness in in-plane (major axis) bending than in out-of-plane (minor axis) bending or the beams which have considerably large laterally unsupported lengths. Unless properly braced against lateral deflection and/or torsion, a slender beam will buckle prior to the attainment of its major axis bending capacity.

Since determining the lateral torsional buckling load or moment of a slender beam is crucial in their design, many studies have been conducted on beam buckling. However, due to the fact that the beam buckling equations are much more complex than the column buckling equations, most of the analytical studies in

Abbreviations: VIM, Variational iteration method; VIA, variational iteration algorithm.

literature are concentrated on simple cases. The solutions for simple buckling problems can be obtained from well-known structural stability books, such as Timoshenko and Gere (1961), Chajes (1974), Wang et al. (2005) and Simitzes and Hodges (2006). In recent years, the advent of computer-aided numerical techniques has enabled the researchers to obtain solutions for more complex lateral buckling problems.

The variational iteration method (VIM) is a kind of nonlinear analytical technique which was proposed by He (1999) and developed fully in the following year. The technique was successfully applied to various kinds of nonlinear problems (He, 2000, 2007; He et al., 2007) since 1999. According to He et al. (2010), the number of publications on VIM has reached 130 in October, 2009, which clearly verifies the effectiveness of the technique in solving nonlinear problems. Very recently, VIM is also applied to the buckling problems. Coskun and Atay (2009), Atay and Coskun (2009), Coskun (2010) and Okay et al. (2010) analyzed the elastic stability of Euler columns with variable cross sections under different loading and boundary conditions and verified that VIM is a very efficient and powerful method in analysis of buckling problems of columns with variable cross sections.

In this paper, this powerful analytical technique is applied to two fundamental beam buckling problems: lateral buckling of (a) simply supported narrow rectangular beams with variable rigidities under uniform moment and (b) narrow rectangular cantilever beams with variable rigidities carrying concentrated load at their free ends. Both linear and exponential variations are considered in minor axis flexural and torsional rigidities of the beams. Exact solutions to these problems, some of which are considerably complex, are available in literature only for beams of constant rigidities and some particular cases of linearly tapered beams. To verify the effectiveness of VIM in solving lateral buckling problems, buckling loads/moments for uniform beams with constant rigidities are studied first. Then, the nonuniform cases are studied for each problem separately. In the paper, the effectiveness of the three VIM algorithms, two of which have recently been proposed by He et al. (2010), in solving lateral torsional buckling equations is also investigated.

LATERAL TORSIONAL BUCKLING OF BEAMS

In this section of the paper, first, the basic lateral buckling theory as given in Timoshenko and Gere (1961) will be summarized very shortly and the notation that will be used in the study will be introduced. Then, the differential equations for lateral torsional buckling of beams with two fundamental loading and restraint conditions will be derived.

General beam buckling equations

In order to derive general lateral torsional buckling equations for narrow rectangular beams, we first consider a rectangular beam

subjected to arbitrary loading in *y-z* plane causing its strong-axis bending. The fixed *x, y, z* coordinate system defines the undeformed configuration of the beam, as shown in Figure 1a. Similarly, ξ, η, ζ , coordinate system located at the centroid of the cross section at an arbitrary section of the beam along its length defines the deformed configuration of the beam. As shown in Figure 1b, the deformation of the beam can be defined by lateral (*u*) and vertical (*v*) displacements of the centroid of the beam, which are positive in the positive directions of *x* and *y*, respectively, and angle of twist (Φ) of the cross section, which is positive about positive *z* axis, obeying the right hand rule.

Hence, the displacements illustrated in Figure 1b, are both negative. For small deformations, the curvatures in *xz* and *yz* planes can be taken, respectively, as d^2u/dz^2 and d^2v/dz^2 and the cosines of the angles between the axes can be taken as listed in Table 1. Since the “warping rigidity” of a narrow rectangular beam can realistically be taken as zero, using positive directions of internal moments defined in Figure 2, the equilibrium equations for the buckled beam can be written as follows:

$$EI_{\xi} \frac{d^2v}{dz^2} = M_{\xi}, \quad EI_{\eta} \frac{d^2u}{dz^2} = M_{\eta}, \quad \text{and} \quad GI_t \frac{d\phi}{dz} = M_{\zeta} \quad (1)$$

representing the major axis bending, minor axis bending and twisting of the beam, respectively. In Equation 1, EI_{ξ} and EI_{η} denote the strong axis and weak axis flexural rigidities of the beam, respectively. Similarly, GI_t denote the torsional rigidity of the beam.

Lateral buckling of simply supported rectangular beams in pure bending

Consider a simply supported rectangular beam with variable rigidities $EI_{\xi}(z)$, $EI_{\eta}(z)$ and $GI_t(z)$ along its length *L* (Figure 3).

If the beam is subjected to equal end moments M_o about *x*-axis, the bending and twisting moments at any cross section can be found by determining the components of M_o about ξ, σ, ζ axes. Considering the sign convention defined in Figure 2, and using Table 1, these components can be written as:

$$M_{\xi} = M_o, \quad M_{\eta} = \phi M_o, \quad \text{and} \quad M_{\zeta} = \left(-\frac{du}{dz} \right) M_o \quad (2)$$

Then, the equilibrium equations for the buckled beam (Figure 1b) become

$$\begin{aligned} [EI_{\xi}(z)] \frac{d^2v}{dz^2} &= M_o, & [EI_{\eta}(z)] \frac{d^2u}{dz^2} &= \phi M_o, & \text{and} \\ [GI_t(z)] \frac{d\phi}{dz} &= \left(-\frac{du}{dz} \right) M_o \end{aligned} \quad (3)$$

It is apparent from Equation 3 that *v* is independent from *u* and Φ , which are coupled. Thus, in this problem, it is sufficient to consider only the coupled equations. Differentiating the last equation in Equation 3 with respect to *z* and using the resulting equation to eliminate *u* in the second equation in Equation 3, the following differential equation for the angle of twist of the beam is obtained:

$$\frac{d^2\phi}{dz^2} + \frac{d[GI_t(z)]}{dz} \frac{1}{[GI_t(z)]} \frac{d\phi}{dz} + \frac{M_o^2}{[GI_t(z)][EI_{\eta}(z)]} \phi = 0 \quad (4)$$

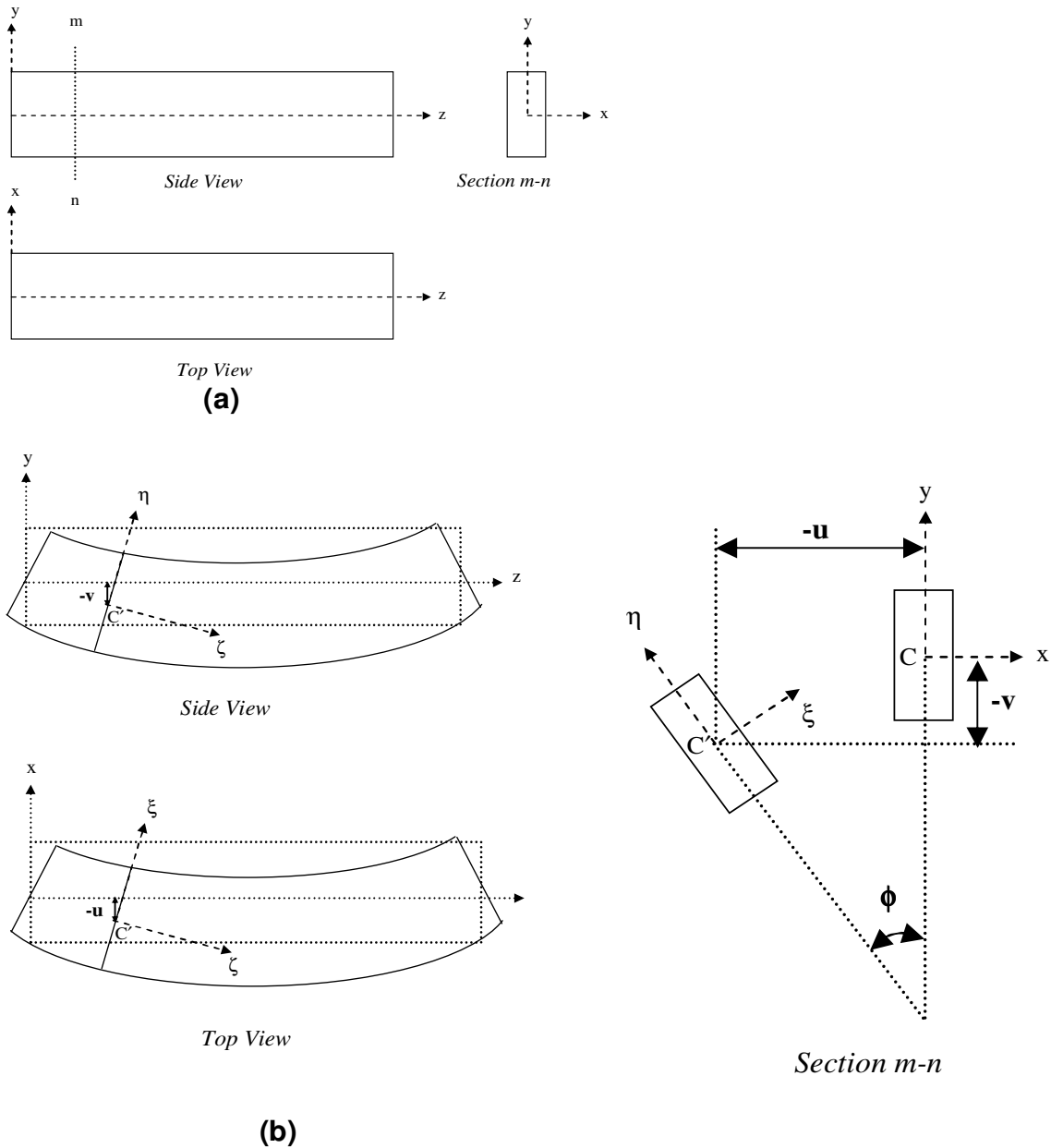


Figure 1. (a) Undeformed and (b) buckled shapes of a double symmetric beam loaded to bend about its major axis.

Since the ends of the simply supported beam are restrained against rotation about z axis, the boundary conditions for the problem are $\xi = 0$ at both $z = 0$ and $z = L$.

Lateral buckling of rectangular cantilever beams with vertical end load

Consider a narrow rectangular cantilever beam of length L with variable rigidities $EI_\xi(z)$, $EI_\eta(z)$ and $GI_t(z)$. If the beam is subjected to a vertical load P passing through its centroid at its free end, as shown in Figure 4, the components of the moments of the load at an arbitrary section $m-n$ about x , y , z axes are

$$M_x = -P(L-z), \quad M_y = 0 \quad \text{and} \quad M_z = P(-u_1 + u) \tag{5}$$

where u_1 is the lateral displacement of the loaded end of the beam as shown in Figure 4b.

Considering the sign convention defined in Figure 2, the bending and twisting moments at this arbitrary section can be written as

$$M_\xi = -P(L-z), \quad M_\eta = -\phi P(L-z) \quad \text{and} \quad M_\zeta = \left(\frac{du}{dz}\right)P(L-z) - P(u_1 - u) [EI_\xi(z)] \frac{d^2v}{dz^2} = -P(L-z) \tag{6}$$

Then, the equilibrium equations for the buckled beam become

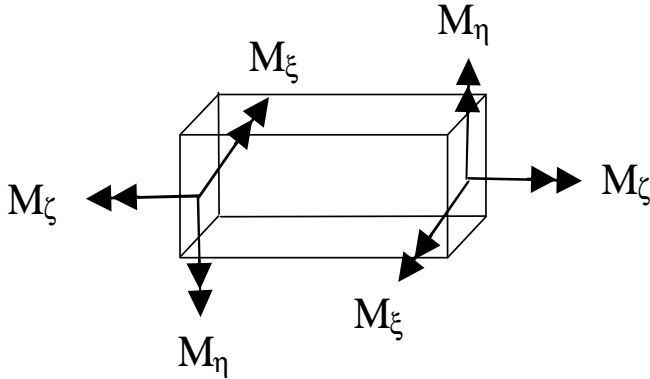


Figure 2. Positive directions for internal moments.

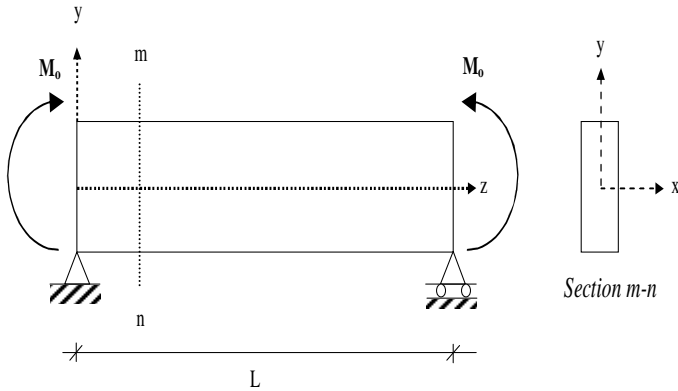


Figure 3. Simply supported rectangular beam under pure bending.

Table 1. Cosine of angles between axes (Timoshenko and Gere, 1961).

| | x | y | z |
|---------|---------|---------|----------|
| ξ | 1 | Φ | $-du/dz$ |
| Φ | $-\Phi$ | 1 | $-dv/dz$ |
| ζ | du/dz | dv/dz | 1 |

$$[E I_\eta(z)] \frac{d^2 u}{dz^2} = -\phi P(L-z) \tag{7}$$

$$[G I_t(z)] \frac{d\phi}{dz} = \left(\frac{du}{dz} \right) P(L-z) - P(u_t - u)$$

Similar to the pure bending case, v is independent from u and Φ . Differentiating the last equation in Equation 7 with respect to z and using the resulting equation to eliminate u in the second equation in Equation 7, the following differential equation is obtained for Φ :

$$\frac{d^2 \phi}{dz^2} + \frac{d[G I_t(z)]}{dz} \frac{1}{[G I_t(z)]} \frac{d\phi}{dz} + \frac{P^2}{[G I_t(z)][E I_\eta(z)]} (L-z)^2 \phi = 0 \tag{8}$$

Since the fixed end of the beam is restrained against rotation and since the twisting moment at the free end is zero, the boundary conditions for this problem are

$$\Phi = 0 \text{ at } z = 0 \text{ and } d\Phi/dz = 0 \text{ at } z = L.$$

VIM FORMULATIONS FOR THE BUCKLING PROBLEMS

In a recent paper, He et al. (2010) proposed three variational iteration algorithms for solving various types of differential equations. The first algorithm is the classical VIM algorithm defined in He (1999). For a general homogeneous nonlinear differential equation,

$$L\phi(z) + N\phi(z) = 0 \tag{9}$$

Where L is a linear operator and N is a nonlinear operator, and the "correction functional" is

$$\phi_{n+1}(z) = \phi_n(z) + \int_0^z \lambda(\xi) \{L\phi_n(\xi) + N\tilde{\phi}_n(\xi)\} d\xi \tag{10}$$

In Equation 10, $\lambda(\xi)$ is a general Lagrange multiplier that can be identified optimally via variational theory, ϕ_n is the n -th approximate solution and $\tilde{\phi}_n$ denotes a restricted variation, that is, $\delta\tilde{\phi}_n = 0$. The iteration algorithm in original VIM, called variational iteration algorithm I (VIA I), is as follows:

$$\phi_{n+1}(z) = \phi_n(z) + \int_0^z \lambda(\xi) \{L\phi_n(\xi) + N\phi_n(\xi)\} d\xi \tag{11}$$

In the second algorithm proposed in He et al. (2010), called variational iteration algorithm II (VIA II), the iteration formula is much simpler:

$$\phi_{n+1}(z) = \phi_0(z) + \int_0^z \lambda(\xi) \{N\phi_n(\xi)\} d\xi \tag{12}$$

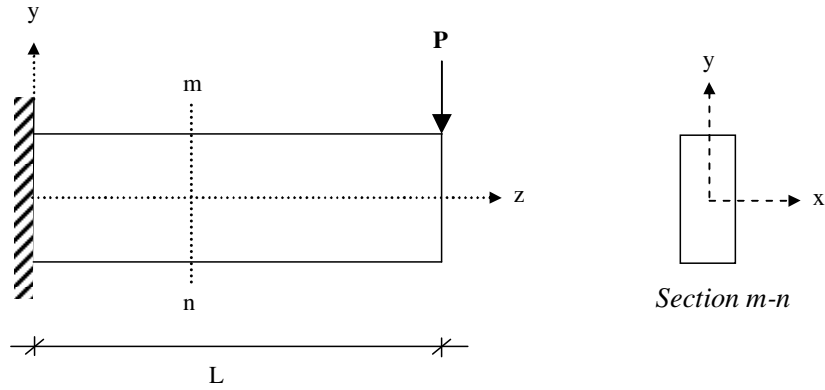
The main shortcoming of this algorithm is stated to be the requirement that ϕ_0 be selected to satisfy the initial/boundary conditions. The third algorithm in He et al. (2010), called variational iteration algorithm III (VIA III), has the following iteration formula:

$$\phi_{n+2}(z) = \phi_{n+1}(z) + \int_0^z \lambda(\xi) \{N\phi_{n+1}(\xi) - N\phi_n(\xi)\} d\xi \tag{13}$$

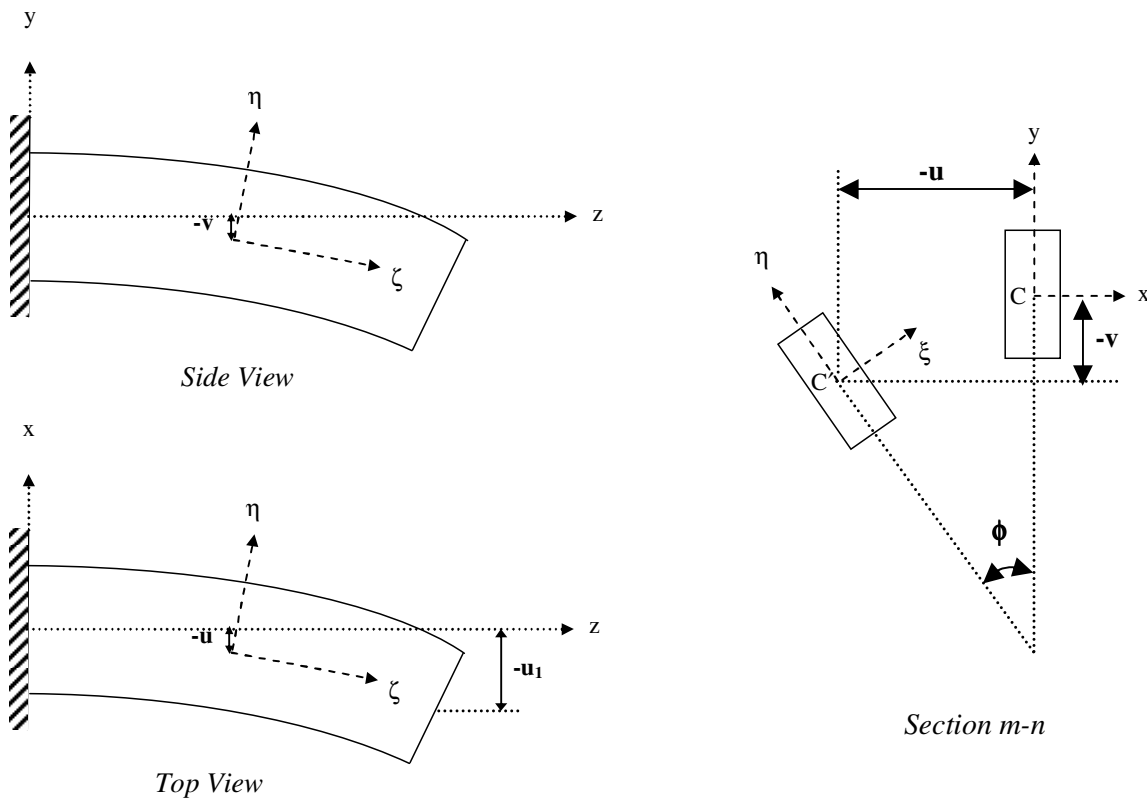
As summarized in He et al. (2010), for a second order differential equation such as the equations of the problems considered in this paper, that is, Equation 4 and Equation 8, $\lambda(\xi)$ simply equals to

$$\lambda(\xi) = \xi - z \tag{14}$$

Thus, the three VIM iteration algorithms for Equation 4 are:



(a)



(b)

Figure 4. (a) Undeformed and (b) buckled shapes of a narrow rectangular cantilever beam carrying concentrated load at its free end.

$$\begin{aligned}
 \phi_{n+1}(z) &= \phi_n(z) + \int_0^z (\xi - z) \{ \phi_n''(\xi) + F(\xi) \phi_n'(\xi) + FM(\xi) \phi_n(\xi) \} d\xi \\
 \phi_{n+1}(z) &= \phi_0(z) + \int_0^z (\xi - z) \{ F(\xi) \phi_n'(\xi) + FM(\xi) \phi_n(\xi) \} d\xi \\
 \phi_{n+2}(z) &= \phi_{n+1}(z) + \int_0^z (\xi - z) \{ F(\xi) [\phi_{n+1}'(\xi) - \phi_n'(\xi)] + FM(\xi) [\phi_{n+1}(\xi) - \phi_n(\xi)] \} d\xi
 \end{aligned}
 \tag{15}$$

$$\begin{aligned}
 \phi_{n+1}(z) &= \phi_n(z) + \int_0^z (\xi - z) \{ \phi_n''(\xi) + F(\xi) \phi_n'(\xi) + FP(\xi)(L - \xi)^2 \phi_n(\xi) \} d\xi \\
 \phi_{n+1}(z) &= \phi_0(z) + \int_0^z (\xi - z) \{ F(\xi) \phi_n'(\xi) + FP(\xi)(L - \xi)^2 \phi_n(\xi) \} d\xi \\
 \phi_{n+2}(z) &= \phi_{n+1}(z) + \int_0^z (\xi - z) \{ F(\xi) [\phi_{n+1}'(\xi) - \phi_n'(\xi)] + FP(\xi)(L - \xi)^2 [\phi_{n+1}(\xi) - \phi_n(\xi)] \} d\xi
 \end{aligned}
 \tag{16}$$

and those for Equation 8 are

In Equation 15 and Equation 16,

Table 2. Normalized buckling moments (α) for the first three modes – constant rigidities.

| Mode # | VIA I | VIA II | VIA III | Exact |
|--------|---------|---------|---------|---------|
| 1 | 9.8696 | 9.8696 | 9.8696 | 9.8696 |
| 2 | 39.4787 | 39.4784 | 39.4784 | 39.4784 |
| 3 | 88.8264 | 88.8264 | 88.8264 | 88.8264 |

$$F(z) = \frac{[G_t(z)]'}{[G_t(z)]}, \quad FM(z) = \frac{M_o^2}{[G_t(z)][E_t(z)]} \quad \text{and} \quad FP(z) = \frac{P^2}{[G_t(z)][E_t(z)]} \quad (17)$$

and prime denotes the differentiation of functions with respect to their variables.

ANALYSIS OF RESULTS

Critical moment for pure bending case

Beams with constant rigidities

If the minor axis flexural and torsional rigidities of the beam are constant; that is, $E_t(z) = E_t$ and $G_t(z) = G_t$, then Equation 4 reduces to the following simpler equation:

$$\frac{d^2\phi}{dz^2} + \lambda_1^2\phi = 0 \quad (18)$$

Where

$$\lambda_1^2 = \frac{M_o^2}{G_t E_t}$$

The solution of Equation 18 is in the form

$$\phi = C_1 \sin(\lambda_1 z) + C_2 \cos(\lambda_1 z) \quad (19)$$

where C_1 and C_2 are constants to be determined from boundary conditions. When the related boundary conditions are used, Equation 19 leads to the following characteristic equation

$$\sin(\lambda_1 L) = 0 \quad (20)$$

whose smallest root yields the first mode critical moment M_{cr} as

$$M_{cr} = \pi \frac{\sqrt{G_t E_t}}{L} \quad (21)$$

Exact values for the second and third modes can be obtained by determining larger roots of Equation 20, which leads to four and nine times the first mode critical moment, respectively.

In order to compare the efficiency of the three variational iteration algorithms mentioned earlier, this case of the problem is solved using all three VIM algorithms. For easier computations, the nondimensional form of the differential equation and the related boundary conditions are written:

$$\frac{d^2\bar{\phi}}{d\bar{z}^2} + \alpha\bar{\phi} = 0 \quad (22)$$

where, $\alpha = \frac{M_o^2 L^2}{G_t E_t}$ with $\bar{\phi}(0) = 0$ and

$$\bar{\phi}(1) = 0$$

where $\bar{z} = z/L$, $\bar{\phi} = \phi$ and α is the “nondimensional critical moment”. For all three algorithms, the initial approximation is chosen as a linear function with unknown coefficients as follows:

$$\bar{\phi} = A\bar{z} + B \quad (23)$$

The coefficients A and B are determined by imposing the boundary conditions to the approximate solution obtained at the end of the iterations, which leads to a characteristic equation whose roots give the buckling moments in different modes. In order to see the convergence of the approximate solutions to the exact solutions, seventeen iterations are conducted for each algorithm and critical moments for the first three modes are computed. It is also worth noting that the function given in Equation 23 cannot satisfy both of the boundary conditions simultaneously.

It is surprising that for this special case of the beam buckling problem, all iteration algorithms yield exactly the same results for the normalized buckling moments, as listed in Table 2, where exact results are also tabulated. Variation of percent errors with iterations plotted in Figure 5 shows how VIM solutions converge to the exact solution. Since all three VIM algorithms give identical results in all iterations, only one plot is presented in Figure 5. As shown in Table 2, VIM solutions are in excellent agreement with the exact results. It is sufficient to perform only five iterations to obtain the exact value of the smallest critical moment. For higher mode values, the number of iterations has to be increased (Figure 5). The excellent match of VIM solutions with the exact results verifies that VIM is a powerful technique in predicting buckling moments of simply supported rectangular beams with constant rigidities under uniform moment and also encourages its use in much more complex beam

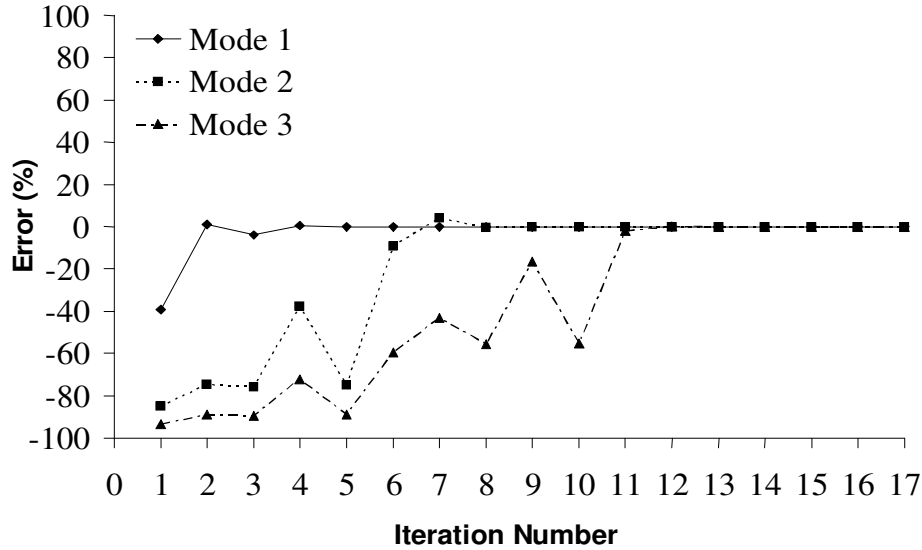


Figure 5. Variation of percent errors in VIM iterations for buckling moments of the first three modes - constant rigidities.

buckling problems, like lateral buckling of beams with variable rigidities.

Beams with linearly varying rigidities

If both the minor axis flexural and torsional rigidities of the beam changes in linear form, that is, if

$$G I_t(z) = G I_t \left(1 + b \frac{z}{L} \right) \quad \text{and} \quad E I_\eta(z) = E I_\eta \left(1 + b \frac{z}{L} \right) \quad (24)$$

where b is a constant determining the “sharpness” of the changes in rigidities along the length of the beam, then, the buckling equation given in Equation 4 takes the following form:

$$\frac{d^2 \phi}{dz^2} + \frac{b}{L + bz} \frac{d\phi}{dz} + \frac{M_o^2}{G I_t E I_\eta} \frac{L^2}{(1 + bz/L)^2} \phi = 0 \quad (25)$$

whose exact solution (Wang et al., 2005) is in the following form:

$$\phi = C_1 \sin(k \ln \eta) + C_2 \cos(k \ln \eta) \quad (26)$$

where, $\eta = 1 + bz/L$ and $k^2 = \frac{M_o^2 L^2}{G I_t E I_\eta b^2}$

When the related boundary conditions are used, the characteristic equation is obtained as follows:

$$\sin(k \ln(1 + b)) = 0 \quad (27)$$

The smallest root of which yields the first mode critical moment M_{cr} as

$$M_{cr} = \frac{\pi b}{\ln(1 + b)} \frac{\sqrt{G I_t E I_\eta}}{L} \quad (28)$$

Exact values for the second and third mode critical moments can be obtained by determining the larger roots of the characteristic equation, which leads to four and nine times the first mode value, respectively. The nondimensional form of Equation 25 can be written as:

$$\frac{d^2 \bar{\phi}}{d\bar{z}^2} + \frac{b}{1 + b\bar{z}} \frac{d\bar{\phi}}{d\bar{z}} + \alpha \frac{1}{(1 + b\bar{z})^2} \bar{\phi} = 0 \quad (29)$$

where $\bar{z} = z/L$, $\bar{\phi} = \phi$ and α is the nondimensional critical moment, as defined in Equation 22.

Since in the case of constant rigidities, all VIM algorithms lead to the same results, the effectiveness of each algorithm is investigated further in this problem. For this purpose, using all VIM algorithms, critical moments for the first three modes are computed for $b=0.3$. In order to see the convergence of the approximate solutions to the exact solutions, thirteen iterations are conducted for each algorithm. Similar to the case of constant rigidities, the iterations are started with the linear approximation given in Equation 23. To simplify the integration processes, variable coefficients in the iteration integrals are

Table 3. Normalized buckling moments (α) for the first three modes – linearly varying rigidities ($b=0.3$).

| Mode # | VIA I | VIA II | VIA III | Exact |
|--------|----------|----------|----------|----------|
| 1 | 12.9043 | 12.9043 | 12.9043 | 12.9043 |
| 2 | 51.6172 | 51.6172 | 51.6172 | 51.6172 |
| 3 | 115.9820 | 115.9820 | 115.9820 | 116.1387 |

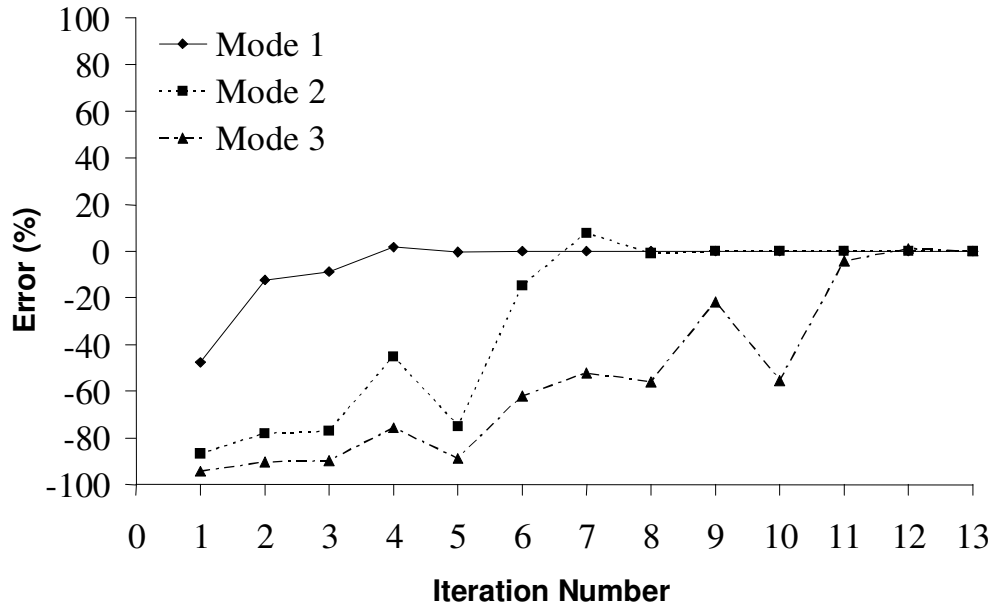


Figure 6. Variation of percent errors with iterations for the first three buckling loads – linearly varying rigidities ($b=0.3$).

expanded in series using nine terms.

Similar to the case of constant rigidities, the different VIM algorithms lead to the same results for buckling moments when $b=0.3$, as listed in Table 3. Variation of percent errors with iterations are also plotted in Figure 6 to show how VIM solutions converge to the exact solution. Since all three VIM algorithms give identical results, only one plot is presented. As shown in Table 3, the agreement between the VIM results and the exact results is considerably good.

Even though all VIM algorithms yield exactly the same results, some important differences are observed between the iteration algorithms in this case as far as the computation time and space are concerned. VIA II is observed to complete the same number of iterations in much smaller amount of time than VIA I and VIA III, for which the computation times are almost identical. VIA II is superior to VIA I and VIA III also in that, its output file takes up less space. The sizes of the output files created by VIA I and VIA III are almost four times larger than that by VIA II. Thus, it can be concluded that VIA II is more effective in solving this kind of differential equations than the other two iteration algorithms. Such differences in computation time and space may occur due to the fact

that VIA I necessitates, in each iteration, second order differentiation of the solution obtained in the previous iteration and VIA III uses, in each iteration, the preceding two iteration results. Furthermore, in VIA I and VIA III, the integral term has to be added to the solution obtained in the previous iteration whereas it is added to the initial approximation in VIA II.

Using VIA II, the normalized buckling moments for other values of b are also computed and plotted in Figure 7, where exact results are also shown. As it is seen from the figure, VIM solutions and exact results are in very good agreement. It is worth noting that the small differences between the results as b increases occurs due to the fact that it is necessary to expand the variable coefficients in the iteration integrals in series using more terms when b is close to one. As the number of terms in series is increased, VIM results are observed to converge to exact results.

Beams with exponentially varying rigidities

If the minor axis bending and torsional rigidities of the beam changes in the following exponential form:

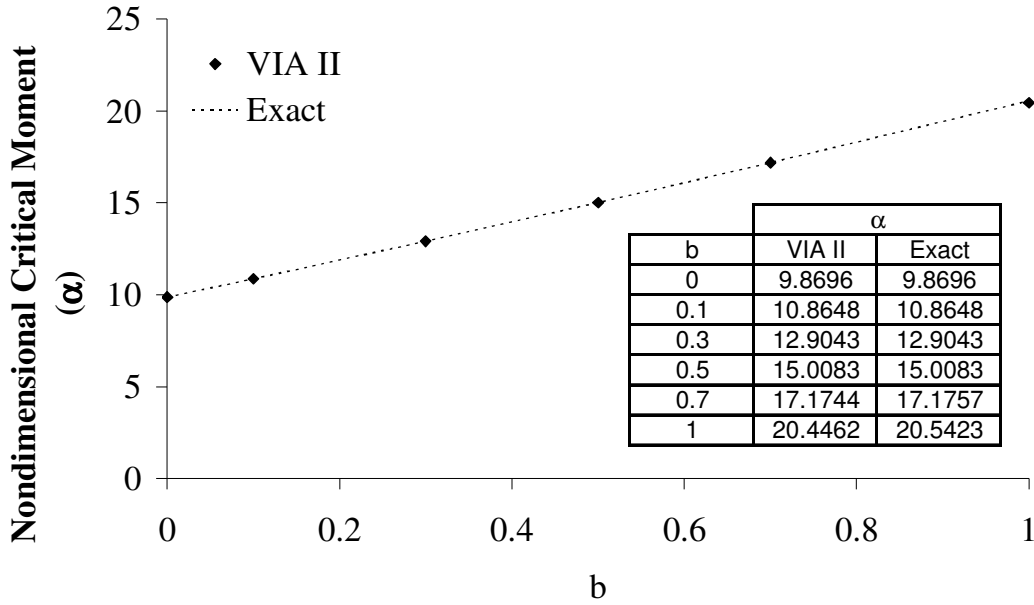


Figure 7. Variation of nondimensional critical moment with “b” values.

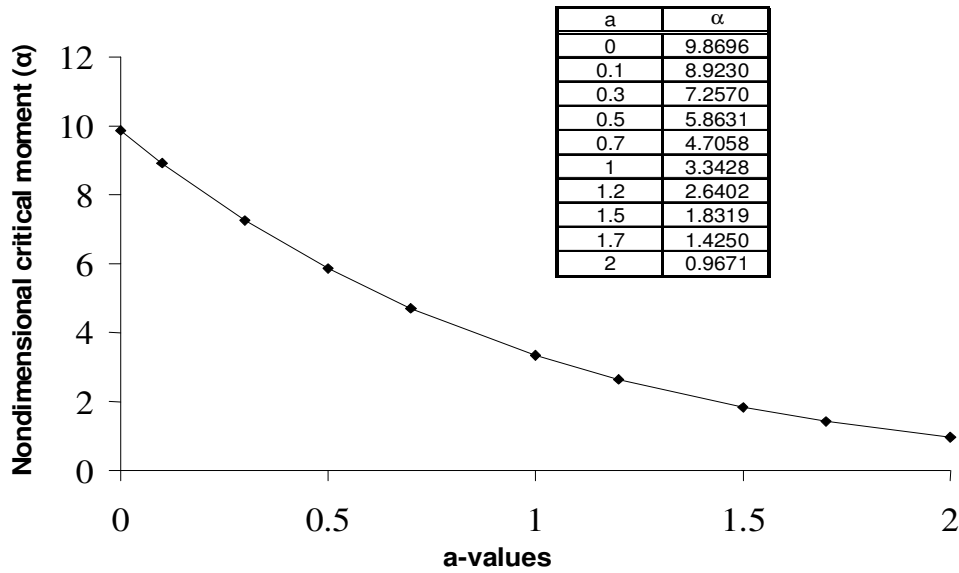


Figure 8. Variation of nondimensional critical moment with “a” values.

$$G I_t(z) = G I_t e^{-a(z/L)} \quad \text{and} \quad E I_\eta(z) = E I_\eta e^{-a(z/L)} \quad (30)$$

where a is a positive constant determining the sharpness of the changes in rigidities along the length of the beam, then, the nondimensionalized form of the buckling equation in Equation 4 become

$$\frac{d^2 \bar{\phi}}{d\bar{z}^2} - a \frac{d\bar{\phi}}{d\bar{z}} + \alpha e^{2a\bar{z}} \bar{\phi} = 0 \quad (31)$$

where $\bar{z} = z/L$, $\bar{\phi} = \phi$ and α is the nondimensional critical moment as defined in Equation 22.

Since in the linear case, VIA II is found to be more effective than VIA I and VIA III, Equation 31 is solved using VIA II for various a values, and the smallest nondimensional critical moments in the first buckling modes are obtained. The results are plotted in Figure 8, which shows how critical moment of a simply supported rectangular beam decreases as a increases.

Table 4. Normalized buckling loads (β) for the first three modes – constant rigidities.

| Mode # | VIA I | VIA II | VIA III | Exact |
|--------|----------|----------|----------|----------|
| 1 | 16.1010 | 16.1010 | 16.1010 | 16.1010 |
| 2 | 104.9830 | 104.9830 | 104.9830 | 104.9830 |
| 3 | 272.7750 | 272.7750 | 272.7750 | 272.7750 |

Even though it can be rather difficult to obtain exact analytical solutions for this particular case of the beam buckling problem, VIM can effectively be used to determine buckling moments in any kind of variations in rigidities, such as the exponential variation studied in this section.

Critical load for cantilever case

Beams with constant rigidities

If the minor axis bending and torsional rigidities of the beam are constant, then Equation 8 reduces to the following simpler equation:

$$\frac{d^2\phi}{dz^2} + \lambda_2^2 (L - z)^2 \phi = 0 \tag{32}$$

Where, $\lambda_2^2 = \frac{P^2}{GI_t EI_\eta}$

Introducing a new variable $s = L - z$, Timoshenko and Gere (1961) obtained the solution of Equation 32 as

$$\phi = \sqrt{s} \left[A_1 J_{1/4}(\lambda_2 s^2 / 2) + A_2 J_{-1/4}(\lambda_2 s^2 / 2) \right] \tag{33}$$

Where $J_{1/4}$ and $J_{-1/4}$ represent Bessel functions of the first kind of order 1/4 and -1/4, respectively. When the related boundary conditions are used to determine the constants A_1 and A_2 , the following characteristic equation is obtained:

$$J_{-1/4}(\lambda_2 L^2 / 2) = 0 \tag{34}$$

The smallest root of this equation is $\lambda_2 L^2 / 2 = 2.0063$ leading to the first mode critical load P_{cr}

$$P_{cr} = 4.0126 \frac{\sqrt{GI_t EI_\eta}}{L^2} \tag{35}$$

observed that the numerical value in Equation 35

changes to 10.2461 and 16.5159 in the second and third mode critical load expressions, respectively. This buckling problem is also solved using all three VIM algorithms. For easier computations, the nondimensional form of the differential equation and the related boundary conditions are written:

$$\frac{d^2\bar{\phi}}{d\bar{z}^2} + \beta(1 - \bar{z})^2 \bar{\phi} = 0 \tag{36}$$

where $\beta = \frac{P^2 L^4}{GI_t EI_\eta}$ with $\bar{\phi}(0) = 0$ and $\frac{d\bar{\phi}}{d\bar{z}}(1) = 0$

where $\bar{z} = z/L$, $\bar{\phi} = \phi$ and β is the “nondimensional critical load”. For all three algorithms, the initial approximation is chosen as given in Equation 23. The coefficients A and B are obtained as defined in pure bending case. Again, in order to see the convergence of the approximate solutions to the exact solutions, seventeen iterations are conducted for each algorithm and critical moments for the first three modes are computed.

Similar to the pure bending case, exactly the same solutions are obtained for critical loads from three different VIM algorithms, as listed in Table 4. Variation of percent errors with iterations are also plotted in Figure 9 to show how VIM solutions converge to the exact solution.

As shown in Table 4 and Figure 9, VIM solutions are in excellent agreement with the exact results. It is to be noted that while it is rather difficult to obtain the critical load from the characteristic equation given in Equation 34, which needs finding the roots of a Bessel function, it is much easier to solve the characteristic equation derived using VIM iterations which are in the form of polynomials. This is one of the advantages of using VIM in this problem, even in the case of constant rigidities.

Beams with linearly varying rigidities

If both the minor axis flexural and torsional rigidities of the beam changes in linear form, that is, if

$$GI_t(z) = GI_t \left(1 - b \frac{z}{L}\right) \quad \text{and} \quad EI_\eta(z) = EI_\eta \left(1 - b \frac{z}{L}\right) \tag{37}$$

where b is a positive constant that can take values between zero and one, then, the buckling equation given in Equation 8 takes the following form:

$$\frac{d^2\phi}{dz^2} - \frac{b}{L - bz} \frac{d\phi}{dz} + \frac{P^2 L^2}{GI_t EI_\eta} \frac{(1 - z/L)^2}{(1 - bz/L)^2} \phi = 0 \tag{38}$$

When larger roots of Equation 34 are obtained, it is

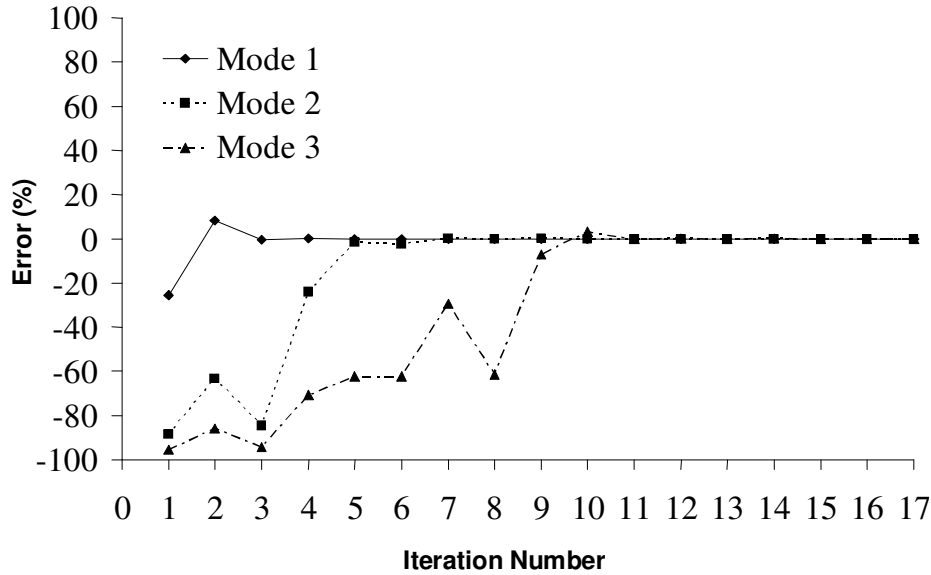


Figure 9. Variation of percent errors with iterations for the first three buckling loads– constant rigidities.

The nondimensional form of Equation 38 can be written as:

$$\frac{d^2\bar{\phi}}{d\bar{z}^2} - \frac{b}{1-b\bar{z}} \frac{d\bar{\phi}}{d\bar{z}} + \beta \frac{(1-\bar{z})^2}{(1-b\bar{z})^2} \bar{\phi} = 0 \quad (39)$$

where $\bar{z} = z/L$, $\bar{\phi} = \phi$ and β is the nondimensional critical moment, as defined in Equation 36.

Since in the case of constant rigidities, all VIM algorithms lead to the same results, the effectiveness of each algorithm on solving Equation 39 is also investigated. For $b=0.5$, the first mode critical moment is computed using each iteration algorithms separately. The iterations are started with the linear approximation given in Equation 23. To simplify the integration processes, variable coefficients in the iteration integrals are expanded in series using twenty one terms. Similar to the earlier studied cases, all algorithms lead to the same result. However, as in the pure moment case, VIA II is more effective than VIA I and VIA III with regard to the computation time and space.

As both the minor axis flexural rigidity and torsional rigidity of a rectangular beam is directly proportional to the height of the beam cross section, a special case of linear variation in beam rigidities occurs when the height of the beam is linearly tapered. Linearly tapered steel beams have wide applications in many engineering applications. They lead to economical designs in laterally-braced cantilever beams with end loading, since under such a loading, the major axis bending moment decreases linearly from the fixed end of the beam to the

free end. However, as shown in Figure 10, which is plotted using VIA II, the buckling load of a laterally-unbraced cantilever beam decreases considerably as b , in other words, the slope of the tapering, increases.

Beams with exponentially varying rigidities

If the minor axis flexural and torsional rigidities of the beam changes in exponential form as given in Equation 30, the nondimensionalized form of the buckling equation in Equation 8 becomes

$$\frac{d^2\bar{\phi}}{d\bar{z}^2} - a \frac{d\bar{\phi}}{d\bar{z}} + \beta e^{2a\bar{z}} (1-\bar{z}^2) \bar{\phi} = 0 \quad (40)$$

where $\bar{z} = z/L$, $\bar{\phi} = \phi$ and β is the nondimensional critical moment, as defined in Equation 36. Since it has already been verified that VIA II is the most effective iteration algorithm for the buckling equations studied in this paper, Equation 40 is solved using VIA II for various values of a . The variation of normalized first mode buckling loads with a is shown in Figure 11. As shown in the figure, the buckling load of a nonuniform cantilever beam with end loading can drop as low as the quarter of its uniform value when a is equal to 2.

Conclusion

In this paper, two fundamental beam buckling problems; lateral torsional buckling of (a) simply supported narrow rectangular beams under uniform moment and (b) narrow

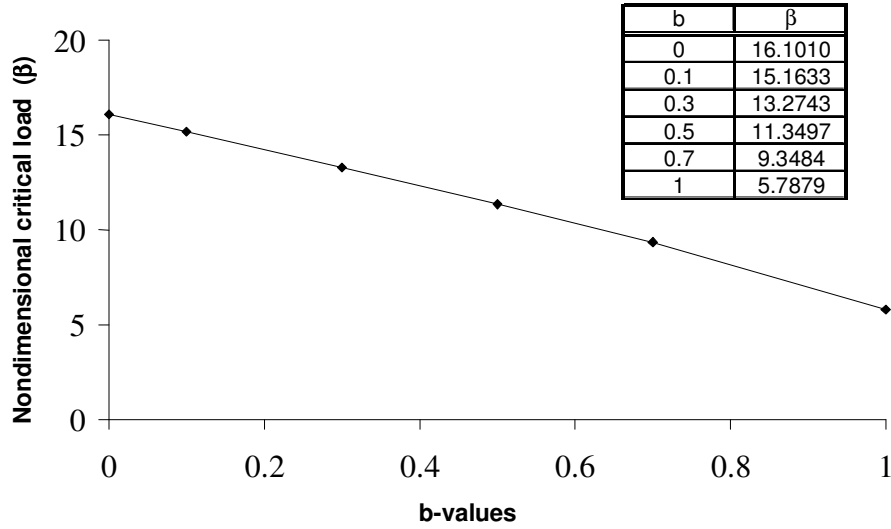


Figure 10. Variation of nondimensional critical load with “b” values.

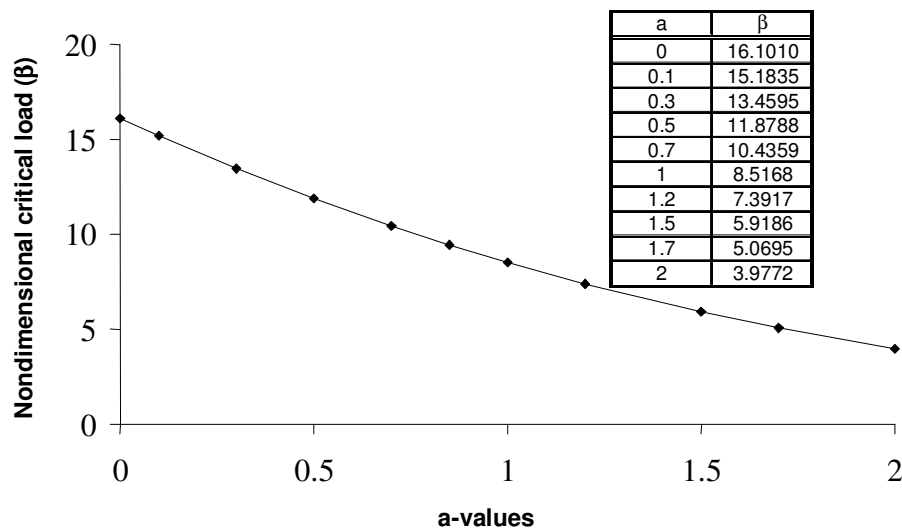


Figure 11. Variation of nondimensional critical load with “a” values.

rectangular cantilever beams carrying concentrated load at their free ends, are studied using variational iteration method (VIM). Exact solutions to these problems are available in literature only for beams of constant rigidities and some particular cases of linearly tapered beams. In order to verify the effectiveness of VIM on solving beam buckling equations and to show the application of the method; firstly, the problems with constant rigidities are studied. The excellent match of the VIM results with the exact results verifies the efficiency of the technique in the analysis of lateral torsional buckling problems. Then, the buckling problems in which the minor axis flexural and torsional rigidities of the beams vary along their lengths are studied. Both linear and exponential variations are considered in nonuniform beams. For the case of variable

rigidities, the differential equations of the studied buckling problems have variable coefficients, which hinder the derivation of exact solutions for these types of problems. However, as shown in the paper, it is relatively easy to write the variational iteration algorithms for these differential equations, which lead to the buckling load/moment of the beam after a few iterations even when the rigidities of the beam change along its length, in exponential form. In the paper, the effectiveness of three VIM algorithms, two of which have been proposed very recently by He et al. (2010), in solving lateral buckling equations was also investigated. Analysis results show that all iteration algorithms yielded exactly the same results in all studied problems. As far as the computation times and spaces are concerned, however, Variational

Iteration Algorithm II (VIA II) is found to be superior than the others especially in problems where the beam rigidities vary along the beam length.

REFERENCES

- Atay MT, Coskun SB (2009). Elastic stability of Euler columns with a continuous elastic restraint using variational iteration method. *Comput. Math. Appl.*, 58: 2528-2534.
- Chajes A (1974). *Principles of structural stability theory*. Prentice Hall, Englewood Cliffs. pp. 211-236.
- Coskun SB, Atay MT (2009). Determination of critical buckling load for elastic columns of constant and variable cross-sections using variational iteration method, *Comput. Math. Appl.*, 58: 2260-2266.
- Coskun SB (2010). Analysis of tilt-buckling of Euler columns with varying flexural stiffness using homotopy perturbation method. *Math. Model. Anal.*, 15(3): 275-286.
- He JH (1999). Variational iteration method - a kind of nonlinear analytical technique: some examples", *Int. J. Non Linear Mech.*, 34(4): 699-708.
- He JH (2000). A review on some new recently developed nonlinear analytical techniques", *Int. J. Nonlinear Sci. Numer. Simul.*, 1(1): 51-70.
- He JH (2007). Variational iteration method – some recent results and new interpretations., *J. Comput. Appl. Math.*, 207 (1): 3-17.
- He JH, Wazwaz AM, Xu L (2007). The variational iteration method: reliable, efficient and promising", *Comput. Math. Appl.*, 54(7-8): 879-880.
- He JH, Wu GC, Austin F (2010). The variational iteration method which should be followed, *Nonlinear Sci. Lett. A*, 1(1): 1-30.
- Okay F, Atay MT, Coskun SB (2010). Determination of buckling loads and mode shapes of a heavy vertical column under its own weight using the variational iteration method, *Int. J. Nonlinear Sci. Numer. Simul.*, 11(10): 851-857.
- Simitses GJ, Hodges DH (2006). *Fundamentals of structural stability*. Elsevier. pp. 251-277.
- Timoshenko SP, Gere JM (1961). *Theory of elastic stability*. Second Edition, McGraw-Hill Book Company, New York.
- Wang CM, Wang CY, Reddy JN (2005). *Exact solutions for buckling of structural members*. CRC Press, Florida. pp. 77-85.